325 REAL-TIME RADAR REFLECTIVITY CALIBRATION FROM DIFFERENTIAL PHASE MEASUREMENTS

Aldo Bellon* and Frédéric Fabry
J. S. Marshall Radar Observatory, McGill University, Montreal, Canada

1. INTRODUCTION

An algorithm for the automatic calibration of the reflectivity measurements of the McGill S-band dual-polarization radar was devised during the 2012 summer season and became ready for real-time implementation in the fall of 2012. This method, based on the consistency between reflectivity and differential phase measurements using a Z_H-K_{DP} relationship from Brandes et al. (2005), is a variation of the one proposed for our radar by Lee and Zawadzki (2006). However, it differs in one important aspect by considering all paths regardless of the intensity of the intervening precipitation, not only those with Φ_{DP} differences exceeding 3º, thus also allowing its application to cases of light precipitation. We had not initially used a three-parameter (Z_H-K_{DP}-Z_{DR}) relationship because it was believed at the time of the publication of the Lee and Zawadzki work that the absolute calibration of our Z_{DR} measurements was unreliable and possessed a high degree of uncertainty due to our fast scanning (6 rpm) radar antenna. However, while running the original algorithm in real-time through this 2013 summer season, the limitations of the two-parameter relationship became more and more evident. We will show that the concern about the quality of our Z_{DR} measurements is no longer valid and that one of the (Z_H-K_{DP}-Z_{DR}) relationships provided by Vivekanandan et al. (2003) yields an excellent agreement between measured and predicted Φ_{DP} differences.

2. PROCEDURE

The S-band 0.8º beam width McGill Doppler radar performs a cycles of 24 rotations at 6 rpm from 0.3 to 32.1 degrees in elevation every five minutes while collecting power and polarimetric measurements at every degree in azimuth and at every kilometer in range. Being situated in a shallow valley, care must be taken to avoid regions that are affected by ground echoes, even though the latter are removed and an interpolation using the surrounding precipitation is performed by our "cleaning" procedure in order to satisfy hydrological considerations.

The consistency between reflectivity and differential phase measurements for the purpose of verifying the calibration of radar power measurements is valid only for paths where precipitation is entirely in liquid form. When testing an algorithm in research mode one can easily choose spatial parameters that would ensure an analysis of only rain echoes for the selected precipitation event(s). However, when dealing in real-time, a more generalized set of filters is required in order to ensure the analysis of "rain-only" echoes at all times. Needless to say, the process of devising these filters evolved during the early stages of the real-time implementation and was not finalized until later in the fall of 2012.

2.1 Algorithm Details

The resulting algorithm can be summarized as follows:

- No analysis is performed if the height of the 0º C isotherm as provided by the Rapid Update Cycle (RUC-2) model forecast is below 2 km.

- Rain paths are taken over four elevation angles (0.5º, 0.9º, 1.4º and 2.2º), along azimuths free of ground echoes and shadows, at heights of at least 0.5 km above the ground and 0.5 km below the bottom of the bright band, and extending up to a maximum range of 115 km. Several hundred rain paths are possible per radar cycle, depending on the horizontal and vertical extent of the precipitation system.

- Rain paths must be at least 20 km long.

- A rain path need not be continuous but may be composed of more than one 'rain' segment.

- A polarimetric target classification scheme originally devised by Vivekanandan et al. (1999) but adapted for our McGill radar has been used to omit any path with non-liquid precipitation such has a rain/snow mix, hail and graupel that may occur in thunderstorms.

- A 5-point (5km) smoother centered over each pixel is applied to the Z_H and Φ_{DP} measurements.

- The theoretical Φ_{DP} difference ($\Phi_{DP\text{-}theor}$) along the path is computed from the integration of the expected specific differential phase differences K_{DP} at each intervening pixel as given by a (Z_H-K_{DP}) relationship based on drop axis ratios suggested by Brandes et al. (2005), namely Z_H=5.7 x 10^4 $K_{DP}^{1.075}$. (See section 2.2)

- The measured Φ_{DP} difference ($\Phi_{DP\text{-}meas}$) is directly obtained from the smoothed values between the end points of the path.

- A path along a given azimuth can contribute only one ($\Phi_{DP\text{-}theor}$, $\Phi_{DP\text{-}meas}$) pair.

- Unlike Lee and Zawadzki (2006) who only considered $\Phi_{DP\text{-}theor}$ > 3º, all paths are kept regardless of the

**Corresponding author address:* Aldo Bellon, J. S. Marshall Radar Observatory, P. O. Box 193, Macdonald Campus, Ste-Anne-de-Bellevue, QC, Canada.
H9X 3V9 E-mail: aldo.bellon@mcgill.ca

intensity of the rain echoes, thus allowing its application to cases of light precipitation.

- $\Phi_{DP\text{-}meas}$ differences which may be negative in light precipitation due to significant noise caused by our fast scanning (6 rpm) radar antenna are not rejected.

- Data from any 5-minute radar cycle with fewer than 50 (selectable) accepted paths are all rejected.

- The set of paths from any 5-minute radar cycle with a ($\Phi_{DP\text{-}theor}$, Φ_{DPmeas}) cross-correlation coefficient γ < 0.4 are all rejected.

- The accepted 5-minute pairs are integrated to produce a set of daily ($\Phi_{DP\text{-}theor}$, Φ_{DPmeas} pairs at 1200 UTC from which the calibration correction is computed.

- The calibration correction ε (to be added to the assumed calibration) is derived from the slope *m* of the least-square fit of the daily ($\Phi_{DP\text{-}theor}$, $\Phi_{DP\text{-}meas}$) pairs as follows:

$$\varepsilon = (10b) \log_{10}(m) \quad (1)$$

where *m* is the slope of the least-square fit and
b = 1.075, the K_{DP} exponent of the selected Z_H-K_{DP} relationship.

- The inclusion of a sufficiently large number of ($\Phi_{DP\text{-}theor}$, $\Phi_{DP\text{-}meas}$) pairs inevitably yields to a reliable estimate of the slope and hence of the calibration. From our real-time and post-analysis experience, ‘sufficient’ should be of the order of one or two thousand, a goal that is easily achievable in most precipitation events of any significance in Montreal.

2.2 Selection of the Z_H-K_{DP} relationship

A Z_H-K_{DP} relationship can be derived by applying a scattering model (Mishchenko et al. 2000) to an assumed drop-size distribution or to a large set of disdrometric data. A parameter required by such model is the amount of deformation with drop size, but the precise dependence is uncertain. Fig. 1 shows the resulting Z_H-K_{DP} relationships deduced from 5 years of disdrometric data in Montreal depending on some of the drop deformation formulas proposed in the literature. We have opted to use the more recent relationship by Brandes et al. (2005). A least-square fit though the corresponding curve yields

$Z_H = 5.7 \times 10^4 K_{DP}^{1.075}$. (2a) or alternatively
$K_{DP} = 3.75 \times 10^{-5} Z_H^{0.93}$ (2b)

3. REAL-TIME RESULTS

The module for the calibration of the reflectivity measurements using the above Z_H-K_{DP} relationship was incorporated into our real-time radar products generation system in late summer 2012 but it required further refinements in order to properly eliminate echoes due to non-liquid precipitation. It became immediately apparent that the quality of the fit between the theoretical and measured Φ_{DP} pairs seemed to depend on the type of precipitation event, namely solely stratiform or a convective-stratiform mix. The former yielded excellent comparisons while an inconsistency was noted for paths with high Φ_{DP} values for events that include some convective precipitation. This discrepancy was initially attributed to an incomplete filtering of non-liquid precipitation present in storm cores but after implementing more stringent filters, the summer season came to an end and thus the problem did not manifest itself for the rest of the year

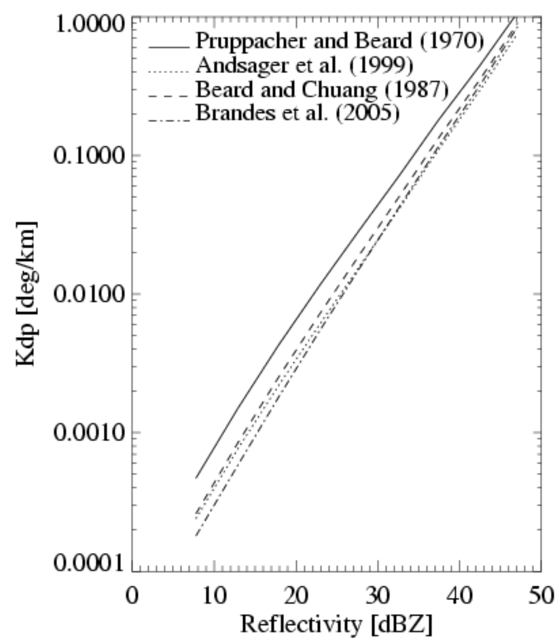

Fig. 1. *Z_H-K_{DP} relationships derived from 5 years of POSS data in Montreal using some of the drop deformation formulas proposed in the literature.*

One welcoming aspect of our technique was that, unlike the recommendation of Lee and Zawadzki (2006), it provided useful results even in situations of light precipitation. The event on the 10-11 May 2013 shown in Fig. 2 illustrates such an excellent example. During that 12-h period of mainly light precipitation 20291 acceptable rain paths where identified. In spite of the large number of paths where $\Phi_{DP\text{-}meas}$ is actually negative, the calibration verification technique still yields useful results because the line of the least-square fit does go through the origin (or very close to it). The slope *m* of the least-square fit (red line) through the scatter plot of all these ($\Phi_{DP\text{-}theor}$, $\Phi_{DP\text{-}meas}$) pairs is 1.056, very close to the 1:1 correspondence (dash blue line), implying a calibration correction ε of just 0.25 dB, well within the expected margin of error of the technique. It is evident that most of the pairs have a

$\Phi_{DP\text{-}theor}$ estimate of less than 2º. If the calibration analysis is performed by considering only the 19695 pairs with $\Phi_{DP\text{-}theor}$ < 2º, the resulting ε remains essentially unchanged at 0.09 dB in spite of the larger scatter as implied by the lower cross-correlation coefficient ɤ=0.543.

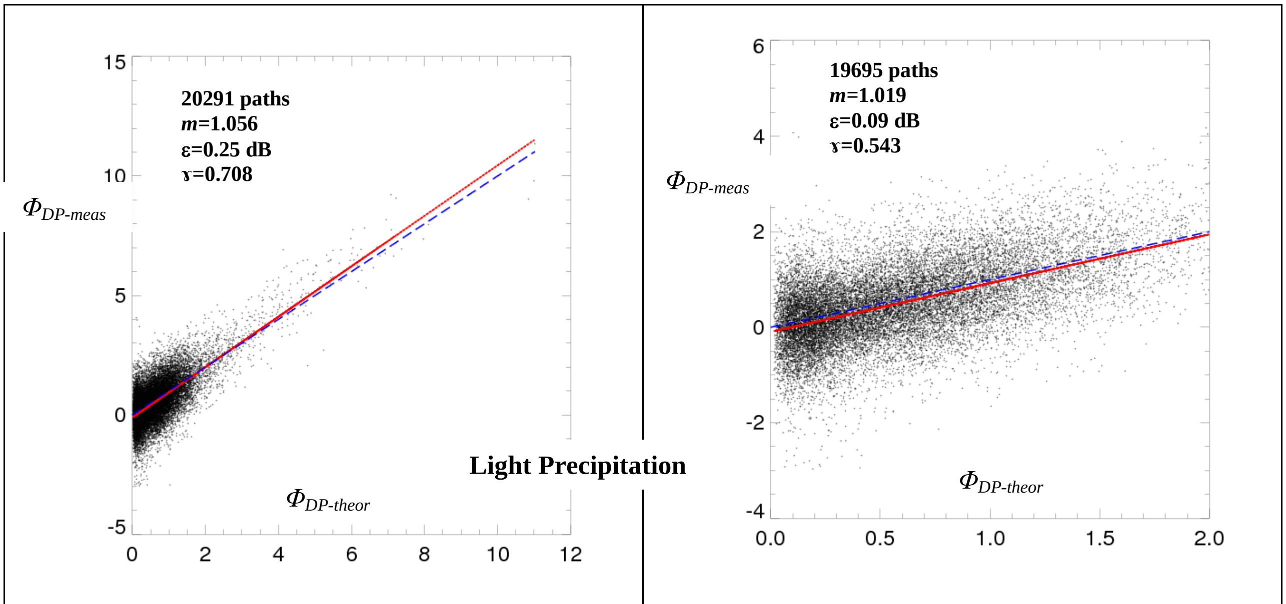

Fig. 2. *Scatter plot of $\Phi_{DP\text{-}meas}$ vs $\Phi_{DP\text{-}theor}$ differences for an event (2219 UTC 10 May to 1024 UTC 11 May 2013) with relatively light precipitation. The red line is the least-square fit while the blue dashed line represents the 1:1 correspondence. The graph on the left considers all the 20291 accepted rain paths yielding a calibration correction ε=0.25 dB while the one on the right considers only those paths with $\Phi_{DP\text{-}theor}$ < 2 º. The resulting ε remains essentially unchanged at 0.09 dB.*

Such near-perfect results did not last long. The onset of the 2013 convective season in Montreal revealed that the discrepancies in the comparison of $\Phi_{DP\text{-}meas}$ and $\Phi_{DP\text{-}theor}$ differences had a more basic origin that the simple inclusion of some non-liquid precipitation as was suspected in late summer 2012. We take the precipitation that occurred over an 11-h period on 22-23 May 2013 as a typical example of the results obtained in a stratiform/convective event in Montreal. The 10253 paths in Fig. 3a reveal a slope that is substantially below the perfect fit from which an apparent overestimation of 0.70 dB would be deduced. However it is apparent even from this scatter plot that it is the paths with the higher Φ_{DP} values that are being overestimated by the assumed Z_H-K_{DP} relationship in (2). In fact the simple separation of the points in this scatter plot in terms of $\Phi_{DP\text{-}theor}$ < 10º (Fig. 3b) and $\Phi_{DP\text{-}theor}$ > 15º (Fig. 3c) underlines the nature of the problem. The 8755 paths with $\Phi_{DP\text{-}theor}$ < 10º reveal a high degree of correlation (ɤ=0.939) and a near-perfect fit with theoretical expectations (ε = -0.09 dB) but those with $\Phi_{DP\text{-}theor}$ > 15º appear to be in a different regime with a least-square fit that would not even pass through the origin and which would imply an overestimation of nearly 3 dB. Similar results were repeatedly encountered throughout the rest of the summer season which necessitated a more thorough investigation to determine the source of the problem.

However, by manually restricting the analysis to a suitably smaller range of $\Phi_{DP\text{-}theor}$ pairs, we were nonetheless able to confirm that our assumed radar calibration was correct throughout the entire period of the experiment, fall 2012 to mid-July 2013.

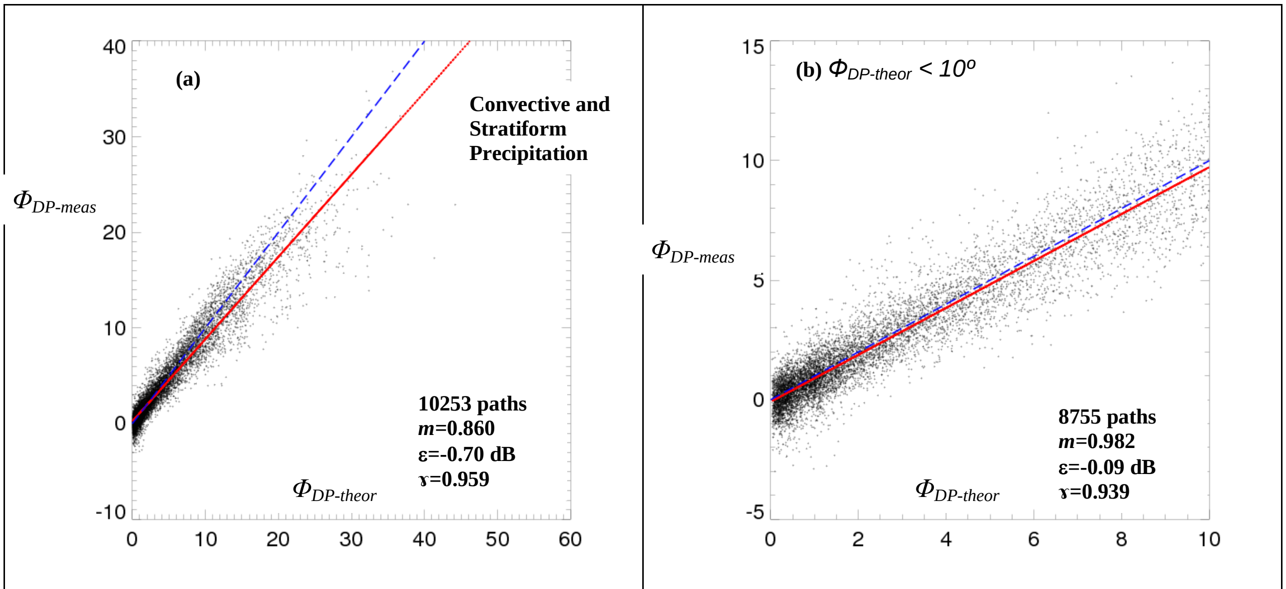

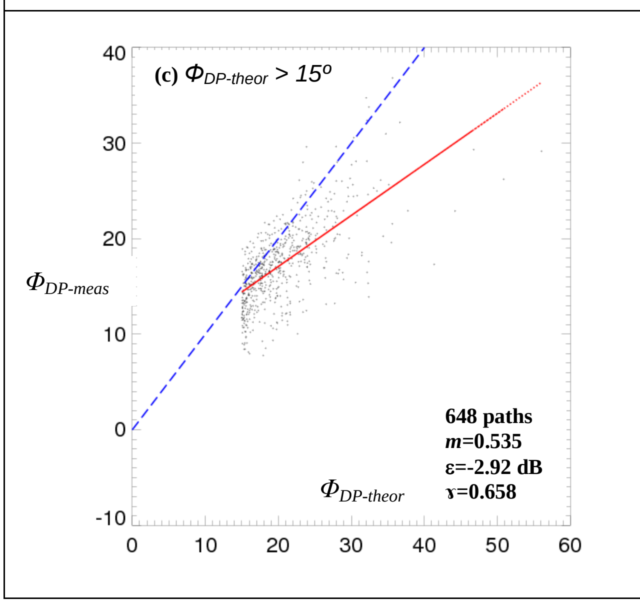

***Fig. 3**. (a): Scatter plot of $\Phi_{DP\text{-}meas}$ vs $\Phi_{DP\text{-}theor}$ differences for an event with convective and stratiform precipitation (2124 UTC 22 May to 0824 UTC 23 May 2013). The least-square fit is distinctively below the 1:1 line yielding an apparent overall calibration correction ε of -0.70 dB (overestimation).*

(b): Scatter plot of the same event but considering only those paths with $\Phi_{DP\text{-}theor} < 10\,^{o}$ and (c) those with $\Phi_{DP\text{-}theor} > 15\,^{o}$.

4. RE-ANALYSIS OF MAY TO JULY 2013 EVENTS

4.1 With the two-parameter Z_H-K_{DP} relationship

An identification of the paths that significantly departed from the 1:1 correspondence immediately revealed that they were usually associated with precipitation cells with not only high reflectivity but also with particularly high Z_{DR} values. Consequently the Φ_{DP} pairs were stratified according to the average Z_{DR} over the path. This average is computed as the ratio of the sum of the horizontal (Z_H) and vertical reflectivity (Z_V) of the rain points within the path, the latter being derived from the smoothed Z_H using the corresponding smoothed Z_{DR} measurements. (A stratification in terms of simply the largest Z_{DR} within the entire path has also been shown to yield essentially similar results). This "Z_{DR}-stratified" calibration analysis algorithm was tested on a variety of events representative of the precipitation that occurred over Montreal during a period from 11 May to 24 July 2013. This sample includes a total of 1061 5-min radar cycles equivalent to 88.4 hours of data and yielding 196277 acceptable rain paths which, as shown in Fig. 4, have been stratified into various Z_{DR} categories. The non-stratified results in Fig. 4a are quite similar to those for the single event illustrated in Fig. 3a, that is, a general overestimation of Φ_{DP} for the intense rain paths and a better match with the predicted values for paths with less intense precipitation. However, the stratification in terms of Z_{DR} appears to be a more efficient discriminator, with Φ_{DP} differences for all paths with an average Z_{DR} of less than 1.4 dB being nearly perfectly predicted by the assumed Z_H-K_{DP} relationship (ε=0.07 dB) but those with moderate average Z_{DR} and in particular those with an average Z_{DR} > 2.1 dB being grossly overestimated by nearly 2 dB. Clearly the selected 2-parameter Z_H-K_{DP} relationship of eq. (2) is no longer valid for these paths. From Fig. 1, it can be seen that the relationship based on drop deformation formula by Andsager et al. (1999) would yield slightly smaller K_{DP} values for the higher reflectivities, but tests have shown that a significant overestimation of the Φ_{DP} differences remains. Moreover, the analysis shown in Fig. 4 emphasizes the necessity of a three-parameter relationship (Z_H-K_{DP}-Z_{DR}) for a proper point K_{DP} estimation and hence of Φ_{DP} differences along a path.

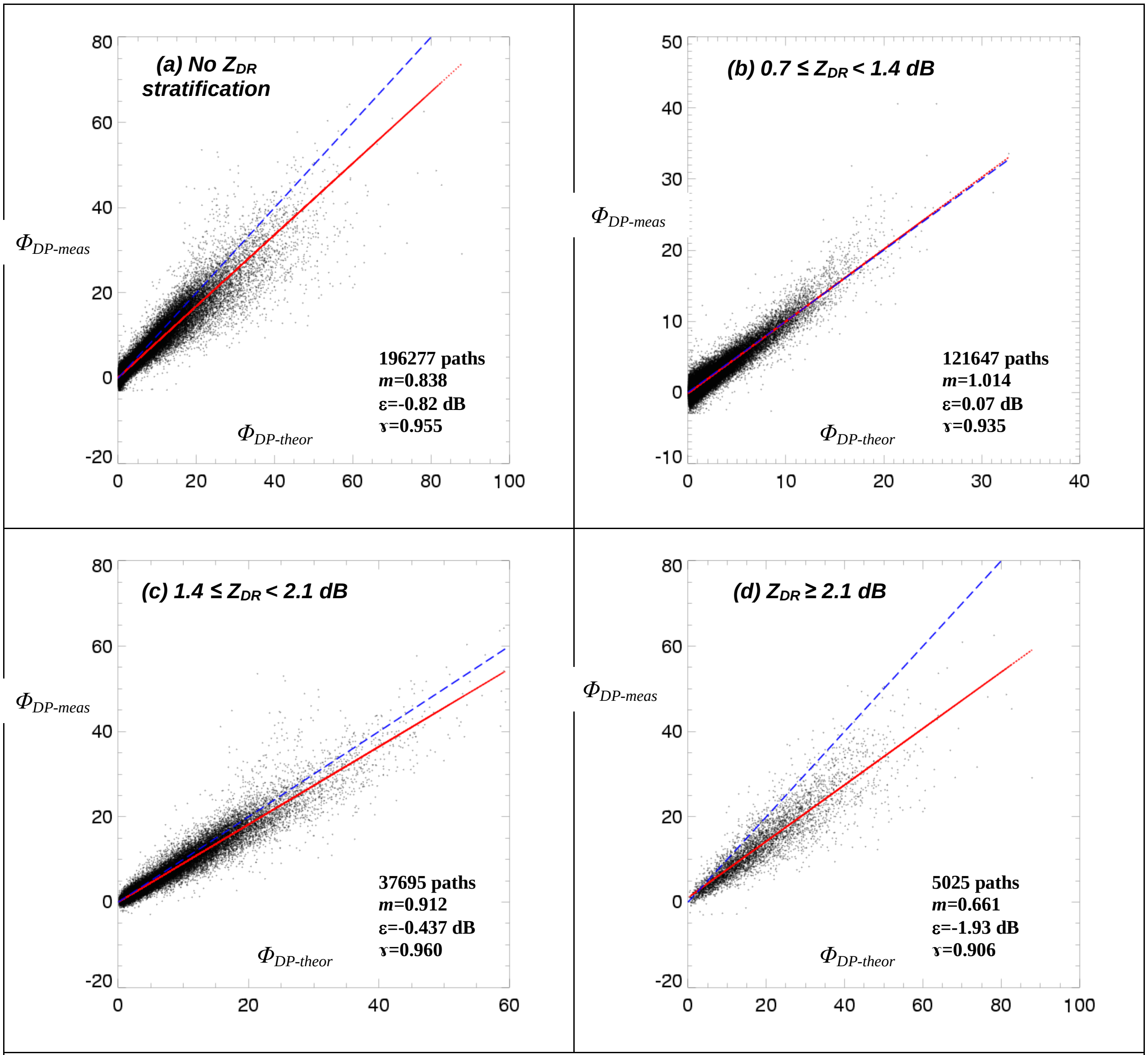

Fig. 4a. *Scatter plot of $\Phi_{DP\text{-}meas}$ vs $\Phi_{DP\text{-}theor}$ differences for the selected events during the period of 11 May to 24 July 2013 (88.4 hours of data). The $\Phi_{DP\text{-}theor}$ differences have been computed using a (Z-K_{DP}) relationship based on Brandes et al. (2005). Scatter plots of $\Phi_{DP\text{-}meas}$ vs $\Phi_{DP\text{-}theor}$ differences for this sample stratified by the average Z_{DR} over each path: (b) 0.7 ≤ Z_{DR} < 1.4 dB, (c) 1.4 ≤ Z_{DR} < 2.1 dB, and (d) Z_{DR} > 2.1 dB*

We have derived the 3-D distribution of the Z_H, K_{DP} and Z_{DR} values from all the rain pixels included in the 196277 rain paths (over 8 million) in order to further illustrate the mutual dependence of these three parameters as measured by the radar. The width of the Z_H, K_{DP} and of the Z_{DR} intervals is 1 dBZ, 0.1 deg/km and 0.1 dB respectively. It will be sufficient to simply show as in Fig. 5 the frequency distribution for a weak differential reflectivity, ($1.4 \leq Z_{DR} < 1.5$ dB), and for a stronger one ($2.8 \leq Z_{DR} < 2.9$ dB) in order to demonstrate that the measured values are mostly centered on the assumed two-parameter relationship (identified by the grey pixels) in the former case while they clearly fall below the expected values in the latter case. As a result, most of the K_{DP} estimates from (2) are positively biased at higher reflectivities and higher Z_{DR}, clearly demonstrating once again the need for a three-parameter relationship.

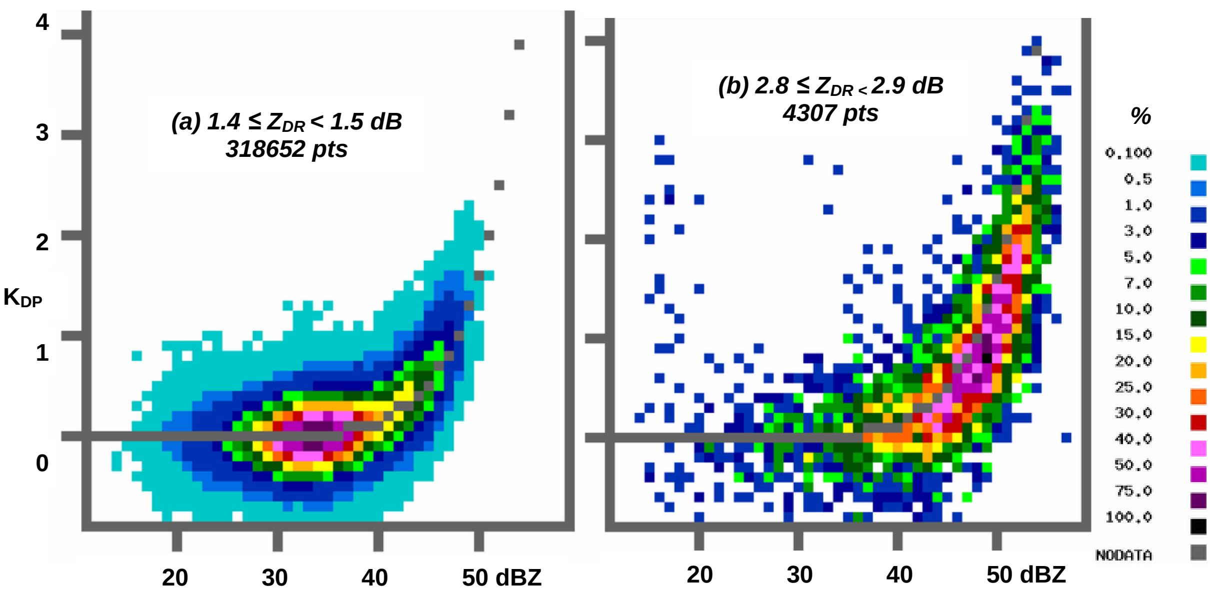

***Fig. 5**. Distribution of the occurrence of measured K_{DP} and of measured Z_H values derived from all the points within rain paths with the indicated 0.1 Z_{DR} interval. The distribution is normalized to 100% at the (K_{DP},Z_H) pair of greatest occurrence for that 0.1 Z_{DR} interval. The grey pixels through the distribution represent the selected Z_H-K_{DP} relationship. Note that most of the points indicate a K_{DP} value that is less than what would be expected from the assumed relationship when Z_{DR} is large.*

4.2 With a three-parameter Z_H-K_{DP}-Z_{DR} relationship

Vivekanandan et al. (2003) have derived three (Z_H-K_{DP}-Z_{DR}) relationships based on different assumptions of drop shapes and of drop size distributions. We have tested all three on our representative 88-h sample of Montreal precipitation. The first two did not yield improved results from the two-parameter relationship (2) but the one that "optimally describes the drop shape versus size relationship for the entire drop diameter range" based on the observations of various previous investigators, (Pruppacher and Pitter (1971), Chandrasekar et al. (1988), Beard and Kubesh (1991) and of Andsager et al. (1999)), showed a remarkable agreement with our data.

$$K_{DP} = 3.32 \times 10^{-5}\, Z_H Z_{DR}^{-2.05} \qquad (3)$$

This relationship is based on the 'corrected' axis ratio relation originally proposed by Brandes et al. (2002), before it was officially corrected in Brandes et al. (2005), and yields more spherical drops for medium and bigger drop sizes, a feature that is also supported by our data presented in Fig.5. Eq. (3) assumes a constrained (two-parameter) gamma DSD. Unlike the relationship in (2b), K_{DP} and Z_H are assumed to be linearly related, with the negative Z_{DR} exponent providing gradually reduced K_{DP} contributions for more intense rainfalls. The results from its application to our 88-h data set are presented in Fig. 6. It is seen that, unlike the results of the corresponding analysis with the two-parameter relationship described in Fig. 4, the measured Φ_{DP} differences better match the

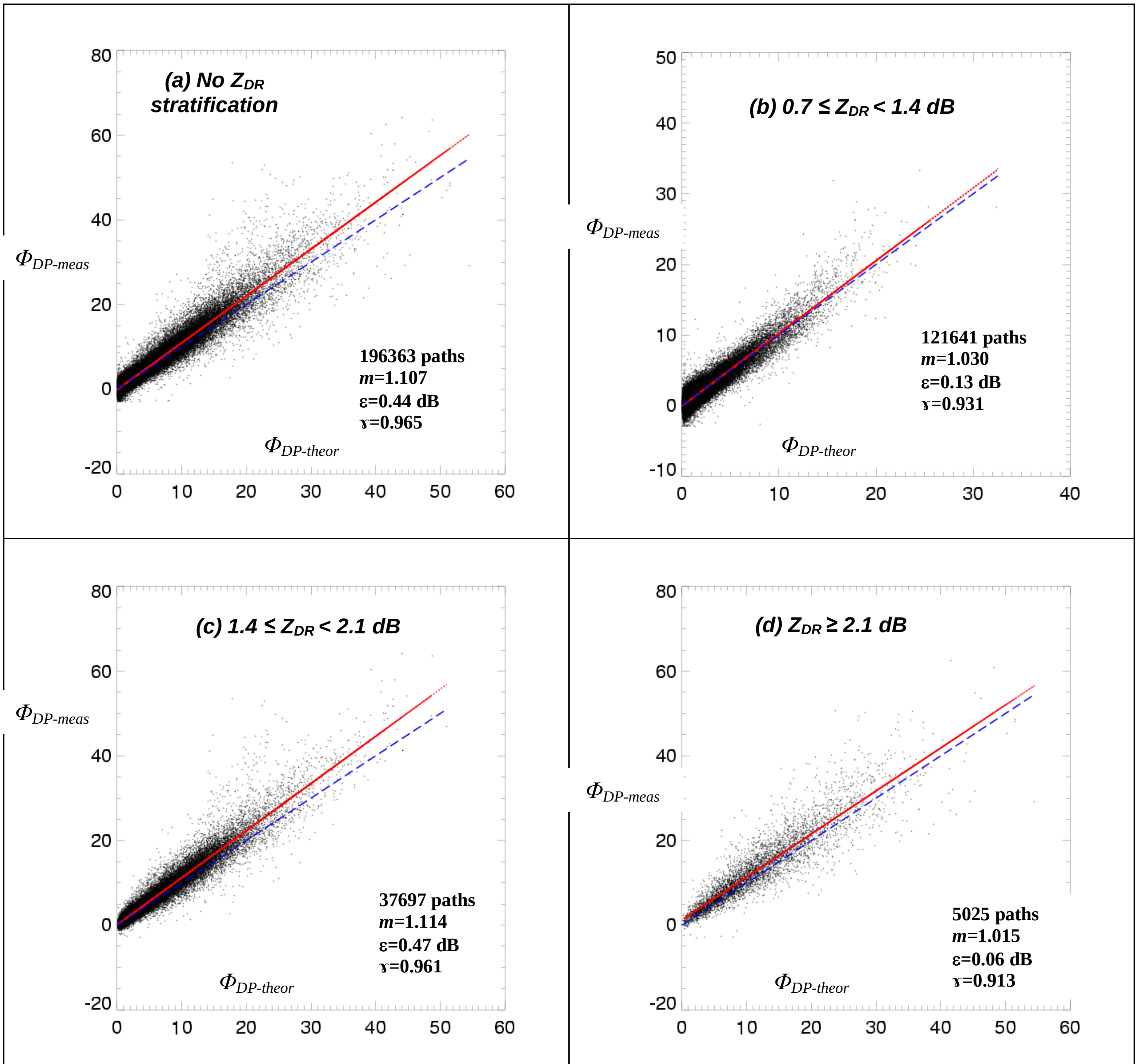

***Fig. 6**. (a) Scatter plot of $\Phi_{DP\text{-}meas}$ vs $\Phi_{DP\text{-}theor}$ differences for all the selected events during the three-month period of Ma to July 2013 (88 hours of data). The $\Phi_{DP\text{-}theor}$ differences have been computed using a (Z_H-K_{DP}-Z_{DR}) relationship derived by Vivekanandan et al. (2003). (b), (c) and (d): Scatter plots of $\Phi_{DP\text{-}meas}$ vs $\Phi_{DP\text{-}theor}$ differences for the three-month sample stratified by the average Z_{DR} over each path. (b) 0.7 ≤ Z_{DR} < 1.4 dB (c) 1.4 ≤ Z_{DR} < 2.1 dB (d) Z_{DR} > 2.1 dB*

theoretical expectations over all ranges of Z_{DR} and hence regardless of the intensity of the intervening precipitation. Because of the assumed linearity between K_{DP} and Z_H in (3), the calibration corrections ε shown in Fig. 6 have been computed from (1) by assuming b = 1.0. However, we point out that any inconsistency with the three-parameter relationship cannot be attributed to either only an error in the measurement of Z_H, or of Z_{DR}, but more likely to a combination of both, thus creating an ambiguity in our quest for a calibration of radar power measurements. Alternatively, it may even be possible, but hopefully highly unlikely, that an excellent agreement could be obtained if the Z_H and Z_{DR} measurements are in error in such a way so as to compensate for each other. The application of (3) to individual events confirmed its general applicability, in particular to the very convective situations of our region. However, it appears to slightly underestimate Φ_{DP} differences of widespread moderate precipitation implying a radar underestimation of the order of 0.5 dB. We must admit that in the original formulation of our technique as described in section 2.1, we did not take into account oxygen and rain path attenuation because it would have indeed caused a greater discrepancy with the two-parameter Z_H-K_{DP} relationship originally proposed but its implementation is now currently under way. Considering that we rarely experience significant attenuation on our S-band radar in our climatic region, the results shown in Fig. 6 are not expected to differ significantly, and may in fact neutralize some of the apparent underestimation deduced in Fig. 6c.

5. SUMMARY AND CONCLUSIONS

A radar calibration procedure based on a Z_H-K_{DP} relationship (2b) derived from a scattering model by assuming a drop axis ratio formula devised by Brandes et al. (2005) has been implemented in real-time on the McGill S-band polarimetric radar in Montreal. The technique of combining the accepted ($\Phi_{DP\text{-}theor}$, $\Phi_{DP\text{-}meas}$) pairs from each 5-min radar cycle into a daily scatter plot from which the slope and hence the calibration correction is computed allows such determination to be achieved even in cases of light precipitation, provided the number of pairs is of the order of 10^3, (Fig. 2). It confirmed the assumed steady calibration of our radar over the entire period of its application, fall 2012 to July 2013. However, the two-parameter Z_H-K_{DP} relationship fails in convective situations yielding larger expected Φ_{DP} differences than what is actually observed with radar, (Fig. 3). A post-analysis of a representative 88-h sample from May to July 2013 inclusive has revealed that this failure occurs mainly along rain paths with large Z_{DR}, (Fig. 4), a fact that has been further corroborated by the 3-D distribution of measured co-located Z_H, K_{DP} and Z_{DR} pixel values along the accepted rain paths, (Fig. 5). The re-analysis of the 88-h sample with a three-parameter Z_H-K_{DP}-Z_{DR} relationship provided by Vivekanandan et al. (2003), given here as Eq. (3), has yielded a much better agreement with the measured Φ_{DP} differences, regardless of the intensity of the precipitation, or of the average Z_{DR} along the rain paths, (Fig. 6). We are thus currently improving our real-time algorithm by adopting the latter equation and furthermore by also considering oxygen and rain path attenuation.

6- ACKNOWLEDGEMENTS

This project was undertaken with the financial support of the Government of Canada provided through the Department of the Environment.

7. REFERENCES

Andsager, K., K. V. Beard, and N. F. Laird, 1999: Laboratory measurements of axis ratios for large drops. *J. Atmos. Sci*., **56**, 2673-2683.

Beard, K. V., and C. Chuang, 1987: A new model for the equilibrium shape of raindrops. *J. Atmos. Sci*., **44**, 1509-1544.

Beard, K. V., and R. J. Kubesh, 1991: Laboratory measurements of small raindrop distortion, Part 2, Oscillations frequencies and modes, J*. Atmos. Sci*., **48**, 2245-2264.

Brandes, E. A., G. Zhang, and J. Vivekanandan, 2002: Experiments in rainfall estimation with polarimetric radar in a subtropical environment. *J. Appl. Meteor*., **41**, 674-685.

Brandes, E. A., G. Zhang, and J. Vivekanandan, 2005: Corrigendum. *J. Appl. Meteor*., **44**, p. 186.

Chandrasekar, V., W. A. Cooper, and V. N. Bringi, 1988: Axis ratios and oscillations of raindrops. *J. Atmos. Sci*., **45**, 1323-1333.

Lee. G. W., and I. Zawadzki, 2006: Radar calibration by gage, disdrometer, and polarimetry: Theoretical limit caused by the variability of drop size distribution and application to fast scanning operational radar data. *J. of Hydrology*, **328**, 83-97.

Mishchenko, M. I., J. W. Hovenier, and L. D. Travis, 2000: Light scattering by nonspherical particles. *Academic Press*, New York, 690 pp.

Pruppacher, H. R., and K. V. Beard, 1970: A wind tunnel investigation of the internal circulation and shape of water droplets falling at terminal velocity in air. *Quart. J. Roy. Meteor. Soc*., **96**, 247-256.

Pruppacher, H. R., and R. L. Pitter, 1971: A semi-empirical determination of the shape of cloud and rain drops. *J. Atmos. Sci*., **29**, 86-94.

Vivekanandan, J., D. S. Zrnic, S. M. Ellis, R. Oye, A. V. Ryzhkov, and J. Straka, 1999: Cloud microphysics retrieval using S-band dual polarization radar measurements. *Bull. Amer. Meteor. Soc*., **80**, 381-406.

Vivekanandan, J., G. Zhang, S. M. Ellis, D. Rajopadhyaya, and S. K. Avery, 2003: Radar reflectivity calibration using differential propagation phase measurement, *Radio Sci*., **38(3)**, 8049, doi:10.1029/2002RS002776,2003